Transportation Research Part C 119 (2020) 102772

Contents lists available at ScienceDirect

Transportation Research Part C

journal homepage: www.elsevier.com/locate/trc

A network-level sidewalk inventory method using mobile LiDAR and deep learning

Qing Hou, Chengbo Ai *

Department of Civil and Environmental Engineering, University of Massachusetts, Amherst, MA, 01003, United States of America

ARTICLE INFO

Keywords:
Asset management
Pedestrian infrastructure
Accessibility
ADA
LIDAR

ABSTRACT

Sidewalks are a critical infrastructure to facilitate essential daily trips for pedestrian and wheelchair users. The dependence on the infrastructure and the increasing demand from these users press public transportation agencies for cost-effective sidewalk maintenance and better Americans with Disabilities Act (ADA) compliance. Unfortunately, most of the agencies still rely on outdated sidewalk mapping data or manual survey results for their sidewalk management. In this study, a network-level sidewalk inventory method is proposed by efficiently segmenting the mobile light detection and ranging (LiDAR) data using a customized deep neural network, i.e., PointNet++, and followed by integrating a stripe-based sidewalk extraction algorithm. By extracting the sidewalk locations from the mobile LiDAR point cloud, the corresponding geometry features, e.g., width, grade, cross slope, etc., can be extracted for the ADA compliance and the overall condition assessment. The experimental test conducted on the entire State Route 9, Massachusetts has shown promising performance in terms of the accuracy for the sidewalk extraction (i.e., point-level intersect over union (IoU) value of 0.946) and the efficiency for network analysis of the ADA compliance (i.e., approximately 6.5 min/mile). A case study conducted in Columbus District in Boston, Massachusetts, demonstrates that the proposed method can not only successfully support transportation agencies with an accurate and efficient means for network-level sidewalk inventory, but also support wheelchair users with accurate and comprehensive sidewalk inventory information for better navigation and route planning.

1. Introduction

Sidewalks play an important role by providing safe paths with exclusive use and uninterrupted flow for pedestrians and wheelchair users. A Federal Highway Administration (FHWA) research conducted by McMahon et al. (2002) shows that the likelihood of a traffic crash with a sidewalk is 88.2% lower than it without a sidewalk. Besides, the existence of the sidewalk leads the drivers to choose lower and safer speeds. A similar study conducted by Ivan et al. (2009) shows that the mean speed is more than seven mph higher for a road without sidewalks than one road with sidewalks. Therefore, public transportation agencies are actively seeking to improve data on existing pedestrian infrastructure to more clearly understand the needs for maintenance and construction of pedestrian facilities. This would allow them to provide equitable accommodation for all modes of transportation.

To meet the obligation of the development of the Americans with Disabilities Act (ADA) Transition Plan and to make informed investment decisions in transportation asset management, public transportation agencies are responsible for timely identification and maintenance of inadequate sidewalks in their jurisdictions. In particular, the ADA Application Guideline (ADAAG) specifies a collection of key feature parameters for pedestrian infrastructure, including sidewalk width, cross slope, grade, curb ramp slope,

* Corresponding author.
E-mail addresses: qhou@umass.edu (Q. Hou), chengbo.ai@umass.edu (C. Ai).

https://doi.org/10.1016/j.trc.2020.102772
Received 23 December 2019; Received in revised form 10 August 2020; Accepted 20 August 2020
Available online 1 September 2020

etc. (Department of Justice, 2010). Unfortunately, these timely evaluation and maintenance activities are often lacking due to the labor-intensive and cost-prohibitive manual data collection process in the current practice.

Although many sidewalk inventories have been successfully implemented by local and state transportation agencies (Illinois Department of Transportation, 2016; New Jersey Department of Transportation, 2007; Loewenherz, 2010), it is identified that the implemented inventory contains limited information. Moreover, productivity is constrained by the limited applications of emerging technologies and the lack of automated or semi-automated methods. Therefore, most of the inventories have been focused only on a small scale, and a network-level assessment of the complete ADA compliance has been lacking. With the recent advancement of remote sensing technologies, many mobile systems with high data acquisition frequency and measurement accuracy, e.g., video log imagery, mobile LiDAR, etc., have become cost-friendly and commercially available with better data quality. In this study, a sidewalk inventory method using mobile LiDAR and deep learning is proposed to address the identified challenges, including (1) a sidewalk inventory framework that leverages the emerging mobile LiDAR and deep learning and can operate at a network-level; (2) a new deep learning model implementation based on PointNet++ for efficiently segmenting LiDAR point clouds; (3) a stripe-based piece-wise principal component analysis (PCA) for accurately extracting sidewalk and conducting the corresponding geometry measurement for ADA compliance. The proposed method is validated and tested on a large real-world network in Massachusetts. To demonstrate the performance and application of the proposed method, a case study of pedestrian accessibility was also conducted. While this case study only focused on the presence and condition of sidewalks, the proposed method can be readily integrated with the detection methods for other critical accessibility infrastructure, such as steps, curb ramps, etc., to facilitate comprehensive accessibility analysis and wheelchair navigation.

The structure of this paper is organized as follows: The background of this study is introduced in Section 1. Literature Review on the road scene segmentation is described in Section 2. Section 3 depicts the details of the proposed method. Section 4 presents the detailed experimental tests to demonstrate the performance of man-made and natural terrains extraction and the overall performance of the proposed method. A case study, which describes the application of the proposed method for wheelchairs in Boston, is also introduced in Section 4. Finally, Section 5 summarizes this study and presents several recommendations for future research.

2. Literature review

The early studies of sidewalk inventory mainly focused on images coupled with a global positioning system (GPS) positioning mechanism. Most of these studies dealt with the localization of the pedestrian infrastructure. A broad spectrum of imagery was attempted to balance the coverage of the network and the granularity of the sidewalk data, mainly including aerial imagery (Guo et al., 2004; Luo et al., 2019), video log imagery (Ai and Tsai, 2016a), crowd-sourcing imagery (Hara et al., 2013, 2014). The major drawback of image-based methods is that the performance is sensitive to the complexity of the scene and the quality of the images. In addition, the spatial information for sidewalks is primarily estimated using photogrammetry, camera calibration, and the integration with the GPS sensor. This type of information can be unreliable or lacking, especially for evaluating ADA compliance.

With the advancements in mobile LiDAR technologies, point cloud data has become more affordable, accessible, and reliable for infrastructure inventory and condition evaluation. There were several initial attempts for inventorying pedestrian facilities and other common urban objects and evaluating their conditions using mobile LiDAR (Ma et al., 2018; Che et al., 2019). As sidewalks and curb ramps are distinguishable by their unique geometrical shapes, e.g., edge, plane, etc. and geometrical measurements, e.g., length, width, adjacency, etc., geometry-based segmentation method has been identified as an efficient and accurate approach. Balado et al. (2018) proposed such a new approach to automatically detect and classify five categories of urban ground elements, including roads, sidewalks, treads, risers, and curbs. Besides the unique geometrical shape and adjacent constraints, many of the road objects, e.g., pavement marking (Gao et al., 2017), signage (Ai and Tsai, 2016b), etc., are also distinguishable because of their unique features captured by LiDAR, e.g., reflectance intensity, etc. Soilan et al. (2018) proposed a method for the detection of road and sidewalk networks by taking advantage of the unique reflectance feature. The urban ground-level, semantic information (e.g., road edges, sidewalks, etc.) can be extracted efficiently through the point cloud pre-processing. Balado et al. (2017) extracted pedestrian facilities, including sidewalks, steps, ramps, etc., from street point cloud data for comprehensive accessibility analysis, using tilt classification in the cross-section based on the k-nearest neighbors (k-NN) search. Besides, the scanning pattern has also been used as strong prior information to facilitate a more efficient process. Ai and Tsai (2016a) proposed a method for sidewalk extraction by taking advantage of the linear scanning pattern of the collected data using a line-scanning LiDAR. Instead of treating the LiDAR point cloud as an arbitrary cluster, the proposed method treated the linear scanning pattern as a continuous sequence with linkage information. Therefore, instead of a 3-D segmentation for all the points, a more straightforward 2-D segmentation for each scan that is perpendicular to the traveling direction was applied. While these LiDAR-based methods have shown promising results, all of these methods are feature-based that bear three significant drawbacks, including (1) they rely on strong priors, e.g., sensor configuration, scene context, etc., to tune the parameters for consistent results; (2) they can only handle simple scenes where features of interest are significant; (3) they rely on iterative (Balado et al., 2018) or sequential search (Ai and Tsai, 2016a) and match strategy for feature extraction that can be time-consuming and infeasible for large-scale data sets. Moreover, a 3-D point cloud often contains a large amount of unorganized and sparsely distributed data points that invalidate immediate applications of many popular images (Gupta et al., 2014; Hariharan et al., 2014) or 2-D point cloud (Wu et al., 2018; Boulch et al., 2018) segmentation techniques.

Therefore, semantic segmentation techniques are often applied and organically split the raw point cloud data into a contextual subset, so that the scale and complexity of the raw point cloud data can be significantly reduced in each subset. To achieve meaningful segmentation in the roadway scenes, many researchers employed region growing algorithms (Jagannathan and Miller, 2007; Vo et al., 2015), and model fitting (Tarsha-Kurdi et al., 2007; Chen et al., 2014) based on some specific geometric or other types

of features. Among them, segmentation based on region growing attempts to grow the neighboring points with some homogeneity geometrical properties from several starting points. Vosselman et al. (2004) extracted bridge, dense vegetation, and building using a surface growing algorithm based on geometrical and color properties. Subwindow was used as the growth unit by Xiao et al. (2013) in the parking lot segmentation. However, these methods are sensitively influenced by the location of initial starting regions and have inaccurate segmentation results due to the worse estimations of the points geometric features near region boundaries. Model fitting segmentation relies on the man-made objects that can be composed into simple geometric shapes such as planes, cylinders, cubes, etc. Barnea and Filin (2013) segmented urban scene based on geometric properties using model fitting. Although these methods have high efficiencies, they are hard to deal with complex objects since they cannot be modeled into easily recognizable geometrical shapes. Some further segmentation methods concentrate on machine learning methods, such as hierarchical clustering (Hu et al., 2013), K-means clustering (Lavoué et al., 2005; Zhang et al., 2008), etc. In the hierarchical clustering algorithm, a hierarchical decomposition of a dataset is created based on some representative geometrical and radiometric features, such as point position and points reflectance. In this process, the point clouds dataset is iteratively split into small subsets until each subset only contains one object. Lu et al. (2016) segmented urban streets by hierarchically clustering the vehicle-mounted, aerial, and stationary laser scanner point clouds. These methods fall out short for processing the points data automatically when facing a large number of point clouds with large scales. In the K-means clustering algorithm, K groups points are obtained from the point clouds dataset using a specific method. The specific method can classify the point clouds dataset by minimizing the sum of squares of distances between the corresponding cluster centroid and points. Yamauchi et al. (2005) proposed a simple frame for clustering mesh normal using in the feature sensitive mesh segmentation. Although these methods demonstrate promising results, they still need to face the problem of long computational time for the large-scale point clouds (Grilli et al., 2017).

Deep learning methods (Su et al., 2018; Jiang et al., 2018; Ye et al., 2018) are increasingly applied on segmenting 3-D point clouds with high efficiency and accuracy. The past segmentation methods classify the data by some heuristic or supervised models based on the most relevant features. These most features, which are related to some LiDAR parameters such as intensity and elevation, are acquired using a feature extraction step based on some previous knowledge. The accuracy is more likely to be lost when these methods deal with the complexity of the terrain (Soilán et al., 2019). However, deep learning methods use the raw data possibly to feed the classifier to minimize the feature handcrafting. Liu et al. (2017) introduced a deep reinforcement learning method to parse the large-scale 3-D point clouds and map the raw data to make the classification. Maturana and Scherer (2015) used VoxNet, a supervised convolutional neural network (CNN) integrating the volumetric grid, to realize the robust object recognition. However, most neural networks do not directly consume the raw point clouds but require preparation, such as voxelization, which can be ineffective. PointNet (Qi et al., 2017a) is a pioneering CNN that directly processes the raw point clouds, which reflects the permutation invariance of the inputting points. PointNet has been popularly applied to semantic segmentation thanks to its high efficiency. Among these applications, Balado et al. (2019) used PointNet to segment road environment from mobile LiDAR system point cloud data. There are two steps in the formulation of PointNet: (1) the spatial encoding of every point is obtained; (2) all individual point features are aggregated to a global point cloud. Although PointNet is an efficient and effective neural network, it cannot capture the local structures which limit PointNet to being applied to complex scenes. The hierarchical neural network, PointNet++ (Qi et al., 2017b), as an extension of PointNet, is introduced to solve this problem thanks to its hierarchy with the PointNet layer (for efficient learning feature locally) and the sampling and grouping layer using the multi-scale, multi-resolution strategy (for abstracting the features globally), which are well suited for the mobile LiDAR point cloud data. It applies PointNet recursively on a nested partitioning of the input point set. PointNet++ can achieve both the robustness under density variation and the preciseness of capturing the local feature details. Due to less appropriate training datasets for some specific purposes, such as extracting man-made terrain, and low accuracy of extracting some small parts in the road environment, such as sidewalk (Behley et al., 2019), few efforts have been made to apply deep learning methods into road scene segmentation. Therefore, in this study, a new deep learning model, PointNet++, is introduced to facilitate the automated sidewalk inventory.

Although studies have been developed and shown promising results in relevant contexts, two unique challenges prevail for the task of LiDAR-based, automated sidewalk inventory on a network level; they are (1) Although sidewalk is man-made objects with a unique planar feature, it can be easily confused by most of the end-to-end detection algorithms as many roadside objects share the same feature; (2) with the dense mobile LiDAR point cloud, a network-level analysis demands an efficient means to handle a large amount of data without degrading the performance. Therefore, this study is aimed at three key methodological contributions to address both challenges, including (1) instead of an end-to-end sidewalk detection model, the proposed method employed the PointNet++ only for segmentation with six specifically-purposed classes that are salient in the roadway scenes; (2) to handle a large amount of point cloud data on a network level, the proposed method introduced a voxel-based down-sampling strategy and the label interpolation method in the new PointNet++ implementation; (3) the proposed method introduced a stripe-based PCA algorithm for precisely extracting the sidewalk regions but using only the man-made and natural terrain class from the segmentation to improve efficiency.

3. Proposed method

3.1. Framework

As identified in the literature review, an automated, network-level sidewalk inventory using the LiDAR point cloud can be challenging, because of the variable density and a large quantity of the LiDAR point cloud, the requirement of accuracy for ADA compliance assessment, and the complicated context of road environments. Therefore, this study proposes a network-level sidewalk inventory framework that consists of three major steps, as shown in Fig. 1.

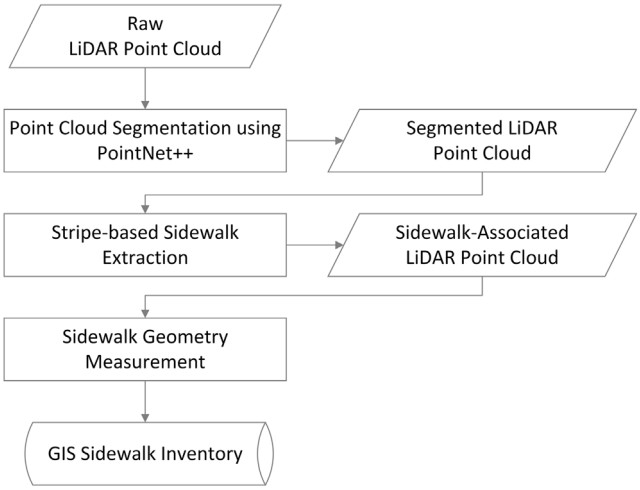

Fig. 1. Overview of the proposed method for sidewalk inventory.

- *Point cloud segmentation*: A new PointNet++ model is implemented to robustly segment the point cloud data into meaningful clusters for the subsequent feature extractions in a generalized road environment, i.e., sidewalk, and the corresponding geometrical measurements. The authors purposely designed the six new classifications for road scenes and only focusing on the man-made and natural terrain as the target for the subsequent process. Such a segmentation process can efficiently and accurately extract the point cloud that shares similar geometrical features, which serves as a robust and generalized regions of interest isolation approach for the subsequent feature extraction and object detection. Therefore, none of the sidewalk-associated point clouds is eliminated for the subsequent step, and yet many of the irrelevant point cloud classes (other than man-made and natural terrain) are significantly reduced.
- *Sidewalk extraction*: A striped-based sidewalk extraction algorithm is developed to extract the sidewalk-associated points reliably. A piece-wise PCA is applied to identify the sidewalk tiles from the point cloud, followed by a longitudinal stitching approach. Under an octree structure, the authors proposed a unified coplanar criterion for the piece-wise PCA method to efficiently split and merge the point clouds that are associated with sidewalks.
- *Geometry Measurement*: A geometry extraction is developed to accurately measure the ADA-compliance-critical measures, including width, cross slope, and grade of the sidewalks, based on the extracted sidewalk-associated point clouds.

3.2. Point cloud segmentation using PointNet++

In this study, PointNet++ is applied to the 3D point cloud segmentation in the road scene. In the PointNet++ model, the point clouds are partitioned into the overlapping local regions by the space distance metric. Then, the local geometrical features extracted from small neighborhoods are clustered into larger groups to produce high-level, generalized features. This process is redone until the features of all the points are obtained.

Fig. 2(a) shows the architecture of the PointNet++ model. The hierarchical architecture mainly contains several set abstraction modules and feature propagation modules. There are a sampling layer, a grouping layer, and a PointNet layer in each set abstraction module, as shown in Fig. 2(b). In the sampling layer, a set of points defining the centroids of local regions from the input points are selected by using farthest point sampling (FPS). In the grouping layer, a point set with a size of $N(d+C)$ and the coordinates of the centroids with the size of $N' \times d$ are inputted. The local region sets are generated by finding the points in the neighborhood of the centroids based on ball query (Har-Peled and Kumar, 2011). The groups of point sets with size $N' \times K \times (d+C)$ are outputted, where K is the number of points in the neighborhood of the centroid points. Each group matches a local region in this layer. In the PointNet layer, the size of the input points in local regions is $N' \times K \times (d+C)$. The local regions are abstracted by encoding local region patterns into feature vectors using a mini-PointNet. An interpolation and a "unit PointNet", which resembles one-by-one convolution in CNNs, are included in each feature propagation module, as shown in Fig. 2(a). The point features of all original points are obtained by propagating the features from the subsampled points to the original points based on distance-based interpolation and across level skip links.

There are many open-source 3-D point cloud datasets (Geiger et al., 2013; Roynard et al., 2018) that can be used to train PointNet++ to segment the road scene. Among these datasets, Oakland 3-D dataset (Munoz et al., 2009) has a small data containing less than 2 million labeled points, which leads to the low accuracy when training the neural networks. Different from the KITTI dataset (Geiger et al., 2013), although the SemanticKITTI dataset (Behley et al., 2019) includes the sidewalk classes that can be directly applied to train PointNet++ to extract the sidewalk dataset, the performance is not ideal with low IoU 0.418. The differences of geometrical features (e.g., elevation offset) between sidewalks and other objects, such as pavement and grass, are not handled

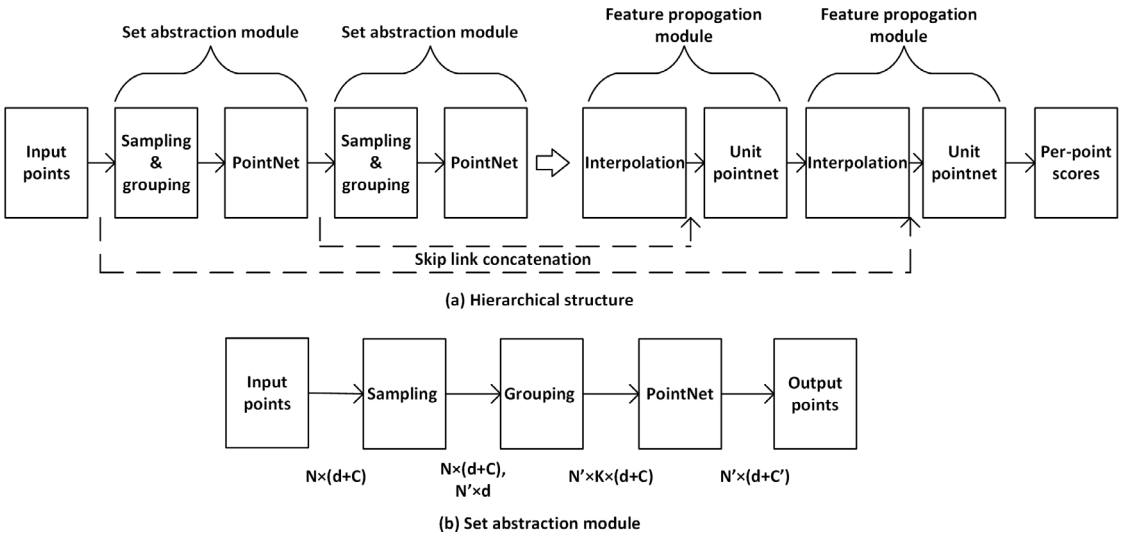

Fig. 2. Overview of the PointNet++ architecture.

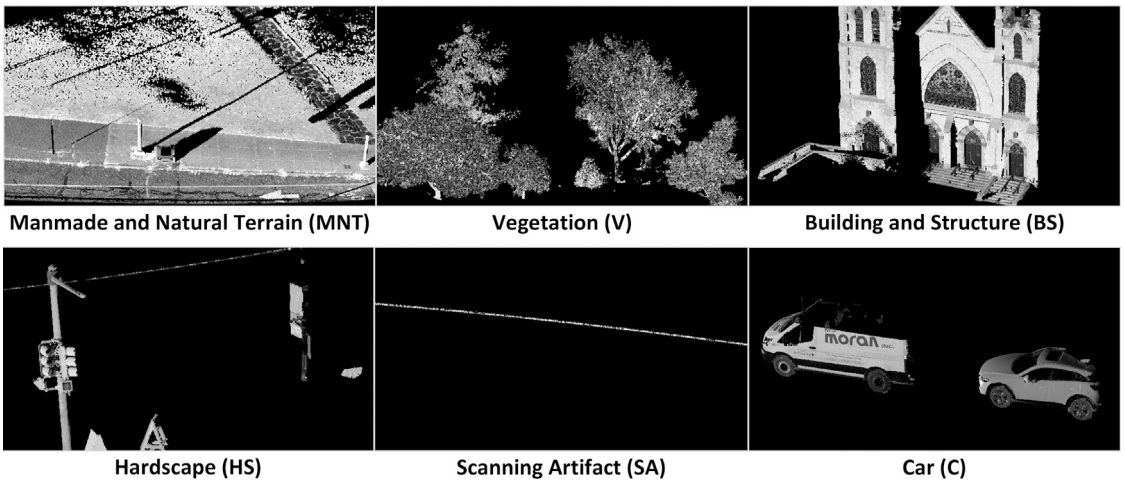

Fig. 3. Examples of the segmentation classes.

well by the CNNs. The semantic3D dataset developed by Hackel et al. (2017) provides a large labeled 3-D point cloud dataset with over 4 billion points in total. This dataset contains eight classes (man-made terrain, natural terrain, high vegetation, low vegetation, buildings, hardscape, scanning artifacts, and cars). These most frequent classes, which have distinguishable features in the road scene, are helpful for the segmentation.

Therefore, in this study, the new PointNet++ model is trained and validated using the semantic3D dataset (Hackel et al., 2017) due to the distinguishable features of the annotated class in this large dataset. For training, based on the semantic3D dataset, the raw LiDAR point clouds are segmented into six customized classes that are salient in most of the road scenes, including man-made and natural terrain, vegetation, building and structure, roadside and roadway object (hardscape), scanning artifacts and cars. Fig. 3 shows examples of the six clusters. The majority of the sidewalk-associated point clouds are included in the man-made and natural terrain class. Therefore, by effectively segmenting the raw point cloud, the subsequent sidewalk extraction algorithm will only need to be applied to the man-made and natural terrain class. Hence, both the complexity of the road scene captured by mobile LiDAR and the scale of the data for the subsequent algorithm to process are significantly reduced.

There are also some other improvements (voxel-based down-sampling and label interpolation) in the newly implemented PointNet++ model when a large amount of point cloud data is processed. Since the total amount of the point clouds in the road environment is extremely large, the voxel-based down-sampling method (Boulch et al., 2018) is introduced to reduce the data size of the point clouds. Compared with other down-sampling methods, such as random down-sampling (Chaperon and Goulette, 2001), k-NN search down-sampling (Beckmann et al., 2015), voxel-based down-sampling can maintain the point clouds distribution while reducing the number of points. To preserve the density variations in a sample, probabilities for selecting the points are based on

the number of points in each three-dimensional bin, called a voxel. Adaptive sampling strategy (Lin et al., 2016), which reduces dilemmas compared with traditional sampling methods, is applied in the voxel-based down-sampling. In adaptive sampling, the selection criteria are adapted based on the preliminary results as the experiment progresses. This type of down-sampling (Orhan and Dekeyser, 2018) includes three basic steps. The first step is to build the voxel container with certain voxel sizes. The second step is to fill the container with the limited samples of points (maximum samples in a voxel container). The points will not be accepted if they are too close together. The third step is to resize the container based on the flatness. The flatness is calculated using PCA. All points will be dropped, but one of them if the surface is flat. Three eigenvectors of each point in the voxel surface are attained by PCA. Each eigenvector represents each axis of the points. The eigenvalue is the square sum of points deviating along the corresponding axis. The eigenvalue describes the variation along the normal direction of the estimated plane. The points in a previous voxel container are sorted and extracted based on the less variation along the normal direction of the estimated plane and the maximum samples of points in a voxel container.

Label interpolation is another improvement used in further label prediction. The sparse points with predicted labels are attained after the prediction using PointNet++ model. The dense points' labels can be acquired by interpolating the labels into the original dense unlabeled points based on the sparse labeled points. The k-NN hybrid search method with a specified radius in the Open3D framework (Zhou et al., 2018) is introduced to interpolate labels. This hybrid search combines the methods of k-NN (Sankaranarayanan et al., 2007) search and fixed-radius search (Behley et al., 2015). K nearest neighbors of the anchor point are effectively found using k-NN search based on three-dimensional Euclidean distance. However, if the points are closely packed together, a small radius of a fixed-radius search can avoid having nearly every point vote. Therefore, the combination of two search methods is applied to acquire the fit neighbors of the anchor point to interpolate the labels. At most k nearest neighbors, which have the distances to the anchor point less than a given radius, are attained using this hybrid search method.

3.3. Stripe-based sidewalk extraction

While many of the existing methods for automated sidewalk extraction using LiDAR point cloud have shown promising results, the 2-D segmentation method developed by Ai and Tsai (2016a) has shown particularly good efficiency without compromising accuracy. However, due to the limited features that can be used from the 2-D profile, the performance of the regression within each 2-D profile varies and often relies on the post-processing for reconnecting the segmented profile longitudinally. In this study, a stripe-based extraction method is proposed to overcome the challenge that 2-D segmentation method encounters. More importantly, the elevation and lateral offset filtering processes that rely on the sensor configuration and the scene context can be effectively removed without impacting the overall performance.

A stripe is defined as the basic processing unit for sidewalk extraction, which covers 3 ft. (approximately 1 meter) in the distance along the traveling direction. All the points associated with the man-made and natural terrain class and bounded by a stripe are converted into an octree structure (Meagher, 1982) and processed in twofold, including:

- *Stripe Splitting*: The split process of the algorithm is to recursively split the point cloud until each node of the octree only contains points that satisfy the coplanar criterion. Figs. 4(a)–(c) shows an illustration of the split process using a 2-D example. Fig. 4(a) shows space contains all point clouds within the stripe as the root node. Since the coplanar criterion is not satisfied, space is split into eight sub-spaces (only four shown in Fig. 4(b)). The point sets in nodes 1 and 2 pass the coplanar criterion, so no further split is required. The point set in node 0 will be further split into eight sub-spaces, as shown in Fig. 4(c). Since the points set in all the nodes pass the coplanar criterion, no further split is required.
- *Stripe Merging*: The merge process of the algorithm is applied to combine the neighboring nodes if the points in the combined node still satisfy the coplanar criterion. The merging process will be exhaustively conducted until no neighboring nodes can be merged without violating the coplanar criterion. Figs. 4(d)–(f) show an illustration of the merging process. As shown in Fig. 4(d), the points in neighboring nodes can share a similar normal direction, which indicates that these points should be merged into the same cluster. Therefore, for each node, the coplanar test is conducted by including the points from one of the neighboring nodes. If the coplanar criterion is satisfied, the two nodes are merged into one, as shown in Fig. 4(e). The merging process is exhaustively conducted for all the nodes until no further merges can be conducted. Fig. 4(f) shows the results of the clustering. Two nodes (i.e., two clusters) are identified in this point cloud.

The coplanar criterion is determined using the PCA. The following equations are constructed for PCA computation for the optimal normal of the given data, i.e., points within a node. The solution is obtained from the three eigenvectors. The eigenvectors represent the three axes of the points, while the eigenvalues denote the square sum of points deviating along the corresponding axis. Therefore, the minimum eigenvalue represents the variation along the normal direction of the best-estimated plane using the points within each node.

$$C \cdot \overrightarrow{v_j} = \lambda_j \cdot \overrightarrow{v_j} \ (j \in 0,1,2) \qquad C = \frac{1}{k}\sum_{i=1}^{k}\left(p_i - \bar{p}\right)\cdot\left(p_i - \bar{p}\right)^T \tag{1}$$

where k is the number of points in the point cloud p_i, $\bar{p}$ is the centroid of the cluster, λ_j is the jth eigenvalue of the covariance matrix C and v_j is the jth eigenvector. Coplanar points should result in minimal variation along the normal direction of the estimated plan. Δ is introduced as the hyperparameter of the coplanar criterion for consistently defining surfaces by tolerating a certain level of noise from the sensor and the interfering objects. Such tolerance is reflected by the eigenvalue along the normal direction, which can be

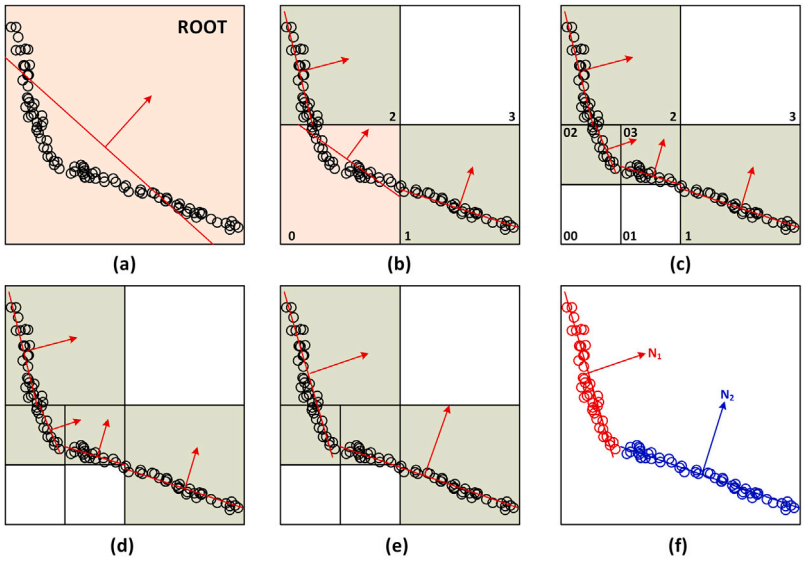

Fig. 4. Illustration of the splitting and merging algorithm.

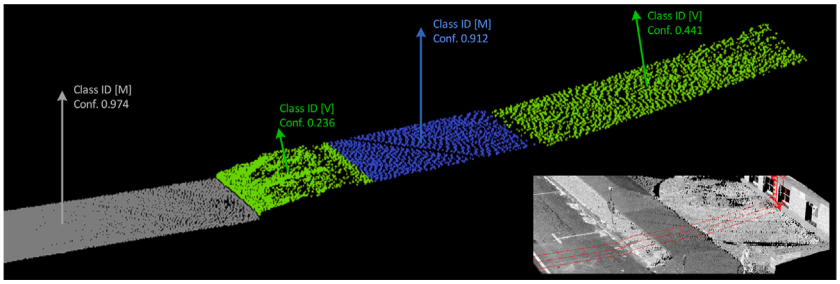

Fig. 5. Illustration of an example stripe-based extraction.

visually explained as the "thickness" of the plane. Therefore, the coplanar criterion is defined as $\lambda_2 \leq \Delta$. In this study, the Δ value of 2 inches was experimentally selected so that the splitting and merging process can be less affected by some of the typical surface disturbances (i.e., road aggregates, grass, etc.) captured by the mobile LiDAR. While other surface estimation and segmentation approaches, such as tilt classification (Balado et al., 2017), can also be applied here for splitting/merging the subspace by normal estimation, the proposed stripe-based PCA method employs a more unified coplanar criterion under an octree structure to efficiently split and merge the point clouds that are associated with sidewalks. Fig. 5 shows an example of the results using the stripe-based sidewalk extraction algorithm. The direction of the arrows shown in Fig. 5 represents the normal direction of the plane, and the magnitude of the arrows represents the confidence level of the extracted plane. It can be observed that the man-made surfaces, e.g., pavement, sidewalk, etc., show a much higher confidence level than the natural surfaces, e.g., grass, where the terrain may slightly distort the surface within the stripe. After all the stripes are processed, the segmentation results are clustered longitudinally based on the k-NN method (Altman, 1992). Subsequently, the key geometry features for a sidewalk include edge-to-edge width, cross slope, grade, etc. Fig. 6 shows an example of the results using the stripe-based sidewalk extraction algorithm, which are the polygons connected from the extracted sidewalk-associated point cloud.

3.4. Geometry measurement

The key features of interest for the sidewalk, including width, cross slope, and grade, are linear features that require continuous measurements. In this study, an interval of 10 ft. was selected for sampling the width and cross slope measurement to balance the detail and redundancy of the measurements, while an interval of 40 ft. was selected for sampling the grade measurement to avoid measuring a local deformation instead of the actual elevation changes along the longitudinal direction.

Each green dot shown in Fig. 7 represents an anchoring point with a fixed interval of 10 ft. At each anchor point, the width is measured between the two intersection points h_1 and h_2. Both points are the intersecting points between the boundary of the detected sidewalk and the vector that is perpendicular to the data collection trajectory (i.e., the yellow line shown in Fig. 7). The x-y

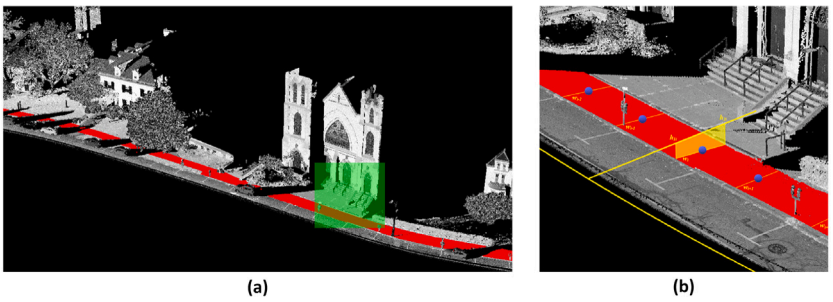

Fig. 6. Illustration of an example for the extracted sidewalk section.

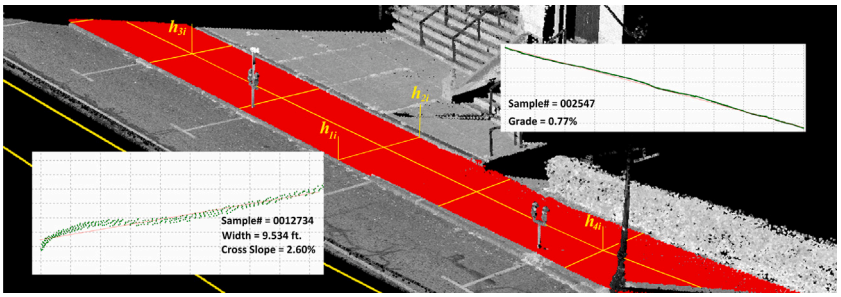

Fig. 7. Illustration of the sidewalk geometry measurements. (For interpretation of the references to color in this figure legend, the reader is referred to the web version of this article.)

distance between h_1 and h_2 are recorded as the width of the sidewalk at the current anchoring point, whereas the linear regression result from all the points between h_1 and h_2 is recorded as the cross slope at the current anchoring point. Similarly, for every four anchoring points (i.e., every 40 ft.), the grade is recorded based on the linear regression results from all the points between h_3 and h_4.

4. Experimental tests

The objective of the experimental tests is to quantitatively evaluate the performance of the proposed method. The experimental tests consist of three parts. Fig. 8 illustrates the extent of the routed in the experimental test. The first part evaluates the performance of the LiDAR point cloud segmentation based on the LiDAR data collected in Northampton, Massachusetts (MA) (green box in Fig. 8); the second part evaluates the overall performance of the sidewalk extraction based on the LiDAR data collected in Northampton and the entire State Route 9 (red line in Fig. 8); the third part shows an application case for the sidewalk inventory results based on the LiDAR data collected in Boston, MA. (blue box in Fig. 8). The mobile LiDAR sensor, Riegl VMZ-2000, which is a line-scanning laser device generating 400,000 laser points per second, was used to collect the data. The scanning line of the LiDAR sensor is aligned horizontally along the ground when the vehicle makes a longitudinal motion on the road. The horizontal scanning range is ±50°, and a 100° fan is generated by the scan to cover the road surface. The frequency of the LiDAR sensor and LiDAR heading angle is configured at 75 Hz and 135°, respectively.

4.1. Performance of the LiDAR point cloud segmentation

In this test, the improved relabeled dataset from Semantic3D was used as the training and validation dataset, containing the six unique classes, including man-made and natural terrain (MNT), vegetation (V), buildings and structures (BS), roadside and roadway object (hardscape) (HS), scanning artifacts (SA) and cars (C). This dataset has been distributed in 75% for training and 25% for validation. The mobile LiDAR point cloud as the testing dataset, which covers a mix of rural and urban road sections and consists of more than 15 million unlabeled points (covering approximately 2 miles of the road scene), was collected on State Route 9 near Northampton, MA.

The results derived from the proposed method were then compared with the ground truth that was manually labeled using a 3-D point cloud processing software, CloudCompare (2018). The training, validation, and testing have been performed on a workstation with Intel(R) Core (TM) i7-8700 CPU, 32 GB RAM, and a GPU NVidia GeForce GTX 1080. Hyperparameters of Max Epochs 500, batch size 16, learning rate 0.001, and momentum 0.9 were selected for balancing the performance and the overall training time. One epoch is a pass through the entire training dataset (Zhang et al., 2016). It was observed that the training model stabilized when epochs reached 500.

Fig. 8. Area map of the tested routes in the experiment tests. (For interpretation of the references to color in this figure legend, the reader is referred to the web version of this article.)

Table 1
Performance of the proposed LiDAR segmentation algorithm.

Weighted IoU	Man-made and natural terrain IoU	Vegetation IoU	Buildings and structures IoU	Hard scape IoU	Scanning artifacts IoU	Cars IoU
0.758	0.932	0.699	0.698	0.104	0.009	0.046

For evaluating the performance of the LiDAR point cloud segmentation, Intersection over Union (IoU) (Tan et al., 2005) was used as the evaluation metric. IoU is the ratio between the intersection and the union of two sets (i.e., result set and ground truth set). It is calculated based on the following equation. An IoU value closer to 1 indicates that the algorithm creates fewer false-positive and false-negative cases.

$$IoU = (result\ set \cap ground\ truth\ set)/(result\ set \cup ground\ truth\ set) \tag{2}$$

Table 1 shows the overall results. Weighted IoU (Zhou et al., 2019), which is weighted by the laser points ratio of each class, is used to investigate the performance of MNT extraction on the full results. Although the PointNet++ model is trained based on the semantic3D dataset, it can be observed that among all the six classes, man-made and natural terrain shows a robust IoU value of 0.932, which provides an ideal input for the subsequent sidewalk extraction algorithm. As the semantic3D dataset for training the PointNet++ model in this study includes different sensor configurations, scene contexts and variable density from the experimental testing dataset, the results clearly demonstrate the transferability of the model that is not dependent on the sensor configurations or scene contexts.

4.2. Performance of the sidewalk extraction

The performance of the sidewalk extraction using the proposed method was evaluated in terms of both accuracy and productivity. Sidewalks were defined and represented differently in previous studies, primarily by polyline (Li et al., 2018) and polygons (López Pazos et al., 2017; Balado et al., 2017). Many transportation agencies adopt the simple polyline representation for efficiency, while many studies adopt the polygon representation for more comprehensive performance evaluations. In this study, both polygon and polyline representations of sidewalk inventory were adopted for revealing the detailed performance of the proposed method and for comparing the performance with the current practices of public transportation agencies, respectively. Two data sets with different scales and different ground truth formats (i.e., sidewalk representations) were prepared, including a 2-mile section of State Route 9 near Northampton, MA, and the entire State Route 9 in Massachusetts (covering 271.76 miles), respectively. The accuracy of sidewalk extraction was quantitatively measured by comparing the results to the manually labeled ground truth. For the 2-mile section, the ground truth was established by manually labeling every LiDAR point that is associated with sidewalks. The IoU for this dataset was defined at the point level, which is depicted by Eq. (2). The proposed method showed a high point-level IoU value of 0.946 that clearly demonstrated the promises for accurate sidewalk inventory. The total extracted sidewalk area within this 2-mile section of the roadway was more than 110,000 yd^2. However, a 2-mile section was insufficient to demonstrate the overall accuracy for network-level analysis. The entire State Route 9 was then prepared as a more comprehensive testing dataset. For the entire State

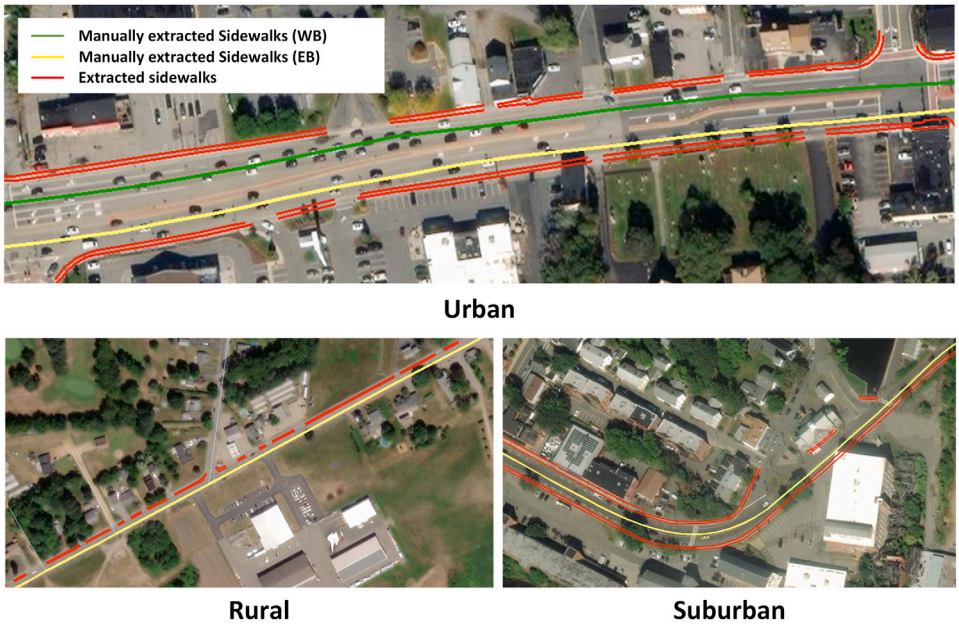

Fig. 9. Illustration of the sidewalk identification results. (For interpretation of the references to color in this figure legend, the reader is referred to the web version of this article.)

Route 9, unfortunately, it was infeasible to establish the ground truth by manually labeling every single LiDAR point due to the labor-intensive nature of data labeling, and the large extent of the dataset. Therefore, the accuracy of the dataset containing the entire State Route 9 was evaluated by a line-level IoU. The ground truth for this dataset was provided by the Massachusetts Department of Transportation (MassDOT) in the format of the polyline layer. Both of the extraction results and the labeled data were linearly referenced to the centerline basemap. Hence, the intersection between the result set and the ground truth set is the overlapping section of the centerline, whereas the union of the result set and ground truth set is both overlapping and non-overlapping section of the centerline. Along the State Route 9 corridor, more than 85 miles of sidewalk locations were identified (covering more than 250,000 yd^2 surface are (a). The proposed method showed a high point-level IoU value of 0.937 that demonstrated the capacity to accurately extract the sidewalk on a network level. It should be noted that the polyline layer for sidewalk inventory by MassDOT was created based on manual digitization from video log images. Therefore, the line-level evaluation shows a slightly smaller IoU value compared with the point-level assessment partially due to the quality of the manual survey results from MassDOT. Subsequently, the geometry measurement of the critical features, including width, cross slope, grade, etc., was successfully carried out at an interval of 10 ft./measurement.

To further investigate the productivity of the proposed method, the computation time for processing the entire State Route 9 in Massachusetts covering 271.76 miles of the road networks was recorded. The proposed method creates the complete sidewalk inventory along the corridor in less than 30 h, from the raw LiDAR point cloud data to the polyline layer of extracted sidewalks, which can be translated into the processing speed of approximately 6.5 min/mile or 0.2 million pts/sec. Fig. 9 shows several examples of the extracted sidewalk visualized by its corresponding edges. Fig. 10 shows a sample section for the sidewalk measurement for ADA compliance.

4.3. Case study - accessibility analysis

The proposed method, consisting of a generalized LiDAR point cloud segmentation and a striped-based sidewalk extraction approach, has shown promising performance in inventorying a large network of sidewalks. A case study was conducted to demonstrate the potential utilization and feasibility of the inventoried sidewalk network with accurate geometry measurements. In this case study, a network of sidewalk in the Columbus Area in the City of Boston was collected using the proposed method, as shown Fig. 11(a). The yellow region is the extracted sidewalks using the proposed method, while the locations A and B are the hypothetical origin and destination of a wheelchair user who plans to attend the local music school from her apartment.

To enable the wheelchair user's uninterrupted travel, the ADAAG (Department of Justice, 2010) and the Proposed Accessibility Guideline for Pedestrian Facilities in Public Right-of-Way (PROWAG) (Architectural and Transportation Barriers Compliance Board, 2011) require that the width of any sidewalk should not reduce below 1.2 m (4 ft.), and the cross slope of any sidewalk should not be greater than 2.0%. These requirements were proposed to ensure the accessibility for wheelchair users. However, in reality, it is challenging to implement these requirements due to the lack of sidewalk inventory information, and more importantly, the lack of detailed and accurate sidewalk geometry information. In the case study, a routing scheme is developed using ArcGIS to identify

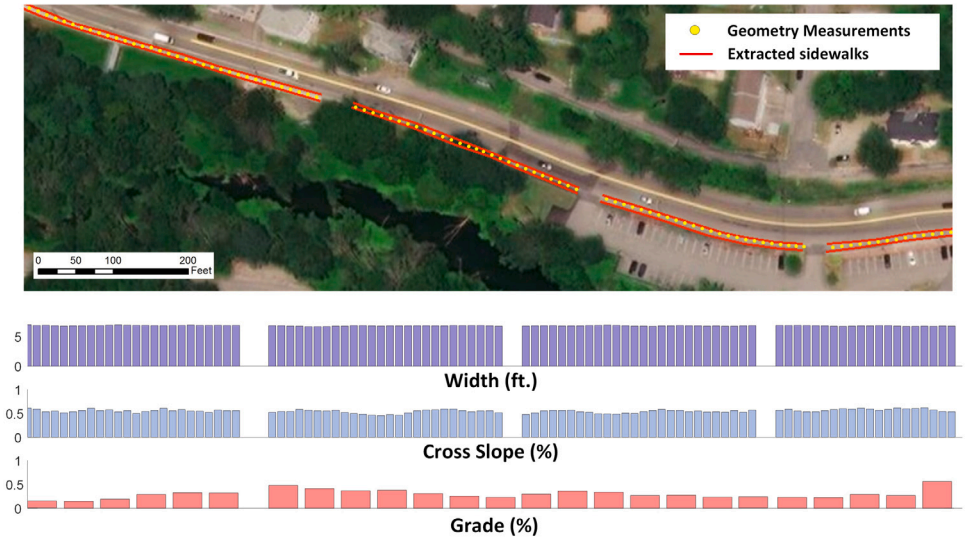

Fig. 10. Illustration of an example for the sidewalk measurements for ADA compliance.

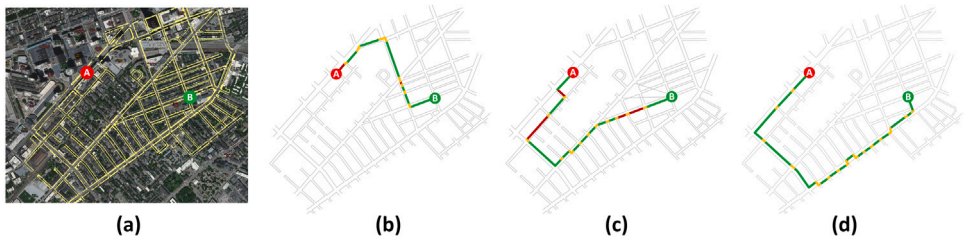

Fig. 11. Illustration of different routing strategies for wheelchair users in the case study. (For interpretation of the references to color in this figure legend, the reader is referred to the web version of this article.)

the shortest path for the wheelchair user to follow from A to B. Three routing scenarios are presented under the conditions of no geometry constraints, with the width constraints and with the cross-slope constraints. It should be noted that this case study focuses only on the presence and conditions of sidewalks, from which the routes were generated. However, there are other facilities and infrastructure, such as steps and curb ramps, that are critical for the wheelchair user's accessibility in the actual scene. The required parameters and compliance of these infrastructure, e.g., a maximum step height of 7 inches (Department of Justice, 2010), etc., can also be programmed for the wheelchair user's route planning and navigation if other step or curb ramp detectors are integrated with the proposed method.

- *Scenario 1 - No Constraints*: If all the sidewalks are in compliance with the ADAGG and PROWAG requirements, the wheelchair user will be able to selected the route based on the connectivity of the available sidewalk links. As shown in Fig. 11(b), the wheelchair user will only need to travel 0.65 miles (1.04 km) from A to B and should be able to reach the destination in less than 16 min at a typical speed of 2.5 mph (4.0 km/h).
- *Scenario 2 - With Width Constraint*: While many sidewalk links are connected, some of the links are not accessible to wheelchair users due to the limitation of the sidewalk width. As the red links shown in Fig. 11(b), several critical sidewalk links become disconnected, which forces the wheelchair users to select a different route, even though the traveling distance will be significantly increased. As shown in Fig. 11(c), the wheelchair user will need to travel 1.11 miles (1.78 km) from A to B and will take more than 30 min to reach the destination.
- *Scenario 3 - With Cross Slope Constraint*: Additional constraints may pose dangerous situations for wheelchair users, especially cross slopes of the sidewalk. As the red lines shown in Fig. 11(c), several critical sidewalk links become unavailable, which forces the wheelchair users to travel even further to reach the destination. As shown in Fig. 11(d), the wheelchair user will need to travel 1.29 miles (2.06 km) from A to B and will take more than 40 min to reach the destination. In addition, due to the longer and more complex route for the wheelchair user to travel, the wheelchair user is also forced to cross more than twice of the crosswalks comparing with the first scenario where no constraints exist (i.e., 19 crossings and eight crossings respectively).

Through the comparison among the three scenarios, it is identified that the sidewalk inventory data with detailed geometry measurement derived by the proposed method can reveal many unavailable or challenging sidewalk links for wheelchair users and

provide them with more realistic and informative route planning. In addition to the prohibitive links that force the wheelchair users to reroute, the detailed geometry measurement will also reveal additional information that helps to understand the level of difficulties for the wheelchair users better. By comparing routes shown in Fig. 11(b) and Fig. 11(c), the wheelchair user may expect to consume more energy, not only because of the longer travel distance but also because of the extra uphill travel along the route. Using the metabolic model developed by Collins et al. (2010), the wheelchair user in Scenario 3 will consume more than four times the energy comparing to Scenario 1. With a large-scale network of inventoried sidewalk that contains detailed geometry measurements derived from the proposed method, it becomes feasible for the city planners and traffic engineers to identify the sidewalk infrastructure that requires maintenance, and more importantly, for the wheelchair users better plan and navigate through a realistic routing for their daily activities.

5. Conclusions and recommendations

Sidewalks are critical to facilitate the essential transportation mode for pedestrians and wheelchair users. While public transportation agencies are actively taking actions for better inspection, maintenance, and management of these critical infrastructures, it remains a challenge to carry out these obligations reliably and efficiently. Although some initial attempts have been made for automated sidewalk extraction so that a network-level inventory will become possible, challenges, such as difficulties in handling complex scenes, dependency on strong priors for sensor configuration and scene context, and the overall inefficiency of the methods, still prevent successful implementation of a network-level inventory.

In this study, a new network-level sidewalk inventory method by leveraging the emerging high-quality mobile LiDAR point cloud data and a deep learning framework are introduced to address the technical challenges. The newly proposed method highlights three major contributions, including (1) a sidewalk inventory framework that leverages the emerging mobile LiDAR and deep learning, and can reliably and efficiently operate at a network-level is proposed; (2) a deep-learning-enabled segmentation method using a newly implemented PointNet++ model that can efficiently reduce the complexity of the road scene in the point cloud; and (3) a stripe-based sidewalk extraction algorithm based on a piece-wise PCA, which can accurately and robustly identify the sidewalk-associated point cloud. The experimental test conducted near Northampton, MA, shows promising results with a point-level IoU value of 0.932. A large-scale test conducted along the entire corridor of State Route 9 in Massachusetts, covering more than 270 miles, shows excellent efficiency with a processing speed of 6.5 min/mile (0.2 million pts/s). The high IoU values that indicate both a high precision rate and a high recall rate of the proposed method, and the high processing speed that indicates high efficiency of the proposed method, demonstrate the promises of the proposed methods for a successful implementation of a network-level sidewalk inventory. A case study conducted in the District of Columbus in Boston, MA, demonstrates the proposed method will provide essential detailed sidewalk inventory information to support better route planning and navigation.

This study not only proposes a new network-level sidewalk inventory method but also lays a strong foundation for LiDAR-based, deep-learning-enabled transportation infrastructure inventory. Further directions of this study include three immediate plans, (1) to implement the proposed method for a large-scale inventory, e.g., statewide inventory, and to further optimize the processing speed through parallel computing; (2) to further improve the existing PointNet++ model for processing other critical infrastructures, such as curb ramp, through transfer learning; (3) to incorporate automated detectors for other critical accessibility facilities and infrastructure, such as steps, to facilitate comprehensive accessibility analysis.

CRediT authorship contribution statement

Qing Hou: Methodology, Software, Formal analysis, Data curation, Investigation, Writing - original draft, Writing - review & editing. **Chengbo Ai:** Conceptualization, Methodology, Software, Writing - original draft, Writing - review & editing, Supervision, Project administration, Funding acquisition.

Acknowledgments

This research was undertaken as part of the Massachusetts Department of Transportation (MassDOT) Research Program with funding from the Federal Highway Administration (FHWA), United States of America State Planning and Research (SPR) funds. The authors are solely responsible for the accuracy of the facts and data, the validity of the study, and the views presented herein.

References

Ai, C., Tsai, Y.J., 2016a. Automated sidewalk assessment method for Americans with disabilities act compliance using three-dimensional mobile lidar. Transp. Res. Rec. J. Transp. Res. Board 2542 (1), 25–32.

Ai, C., Tsai, Y.J., 2016b. An automated sign retroreflectivity condition evaluation methodology using mobile LiDAR and computer vision. Transp. Res. C 63, 96–113.

Altman, N.S., 1992. An introduction to kernel and nearest-neighbor nonparametric regression. Amer. Statist. 46 (3), 175–185.

Architectural and Transportation Barriers Compliance Board, 2011. Proposed Guidelines for Pedestrian Facilities in the Public Right-of-Way. Architectural and Transportation Barriers Compliance Board.

Balado, J., Díaz-Vilariño, L., Arias, P., Garrido, I., 2017. Point clouds to indoor/outdoor accessibility diagnosis. ISPRS Ann. Photogramm. Remote Sens. Spatial Inf. Sci. 4.

Balado, J., Diaz-Vilarino, L., Arias, P., Gonzalez-Jorge, H., 2018. Automatic classification of urban ground elements from mobile laser scanning data. Autom. Constr. 86, 226–239.

Balado, J., Martínez-Sánchez, J., Arias, P., Novo, A., 2019. Road environment semantic segmentation with deep learning from MLS point cloud data. Sensors 19 (16), 3466.
Barnea, S., Filin, S., 2013. Segmentation of terrestrial laser scanning data using geometry and image information. ISPRS J. Photogramm. Remote Sens. 76, 33–48.
Beckmann, M., Ebecken, N.F., de Lima, B.S.P., et al., 2015. A KNN undersampling approach for data balancing. J. Intell. Learn. Syst. Appl. 7 (04), 104.
Behley, J., Garbade, M., Milioto, A., Quenzel, J., Behnke, S., Stachniss, C., Gall, J., 2019. SemanticKITTI: A dataset for semantic scene understanding of lidar sequences. In: Proceedings of the IEEE International Conference on Computer Vision. pp. 9297–9307.
Behley, J., Steinhage, V., Cremers, A.B., 2015. Efficient radius neighbor search in three-dimensional point clouds. In: 2015 IEEE International Conference on Robotics and Automation (ICRA). IEEE, pp. 3625–3630.
Boulch, A., Guerry, J., Le Saux, B., Audebert, N., 2018. Snapnet: 3D point cloud semantic labeling with 2D deep segmentation networks. Comput. Graph. 71, 189–198.
Chaperon, T., Goulette, F., 2001. Extracting cylinders in full 3D data using a random sampling method and the Gaussian image.
Che, E., Jung, J., Olsen, M.J., 2019. Object recognition, segmentation, and classification of mobile laser scanning point clouds: A state of the art review. Sensors 19 (4), 810.
Chen, D., Zhang, L., Mathiopoulos, P.T., Huang, X., 2014. A methodology for automated segmentation and reconstruction of urban 3-D buildings from ALS point clouds. IEEE J. Sel. Top. Appl. Earth Obs. Remote Sens. 7 (10), 4199–4217.
CloudCompare, 2018. CloudCompare User Manual, Version 2.6.1.
Collins, E.G., Gater, D., Kiratli, J., Butler, J., Hanson, K., Langbein, W.E., 2010. Energy cost of physical activities in persons with spinal cord injury. Med. Sci. Sports Exerc. 42 (4), 691–700.
Department of Justice, 2010. ADA Standards for Accessible Design. Department of Justice.
Gao, Y., Zhong, R., Tang, T., Wang, L., Liu, X., 2017. Automatic Extraction of Pavement Markings on Streets from Point Cloud Data of Mobile LiDAR. Meas. Sci. Technol. 28 (8), 085203.
Geiger, A., Lenz, P., Stiller, C., Urtasun, R., 2013. Vision meets robotics: The KITTI dataset. Int. J. Robot. Res. (IJRR).
Grilli, E., Menna, F., Remondino, F., 2017. A review of point clouds segmentation and classification algorithms. Int. Arch. Photogramm. Remote Sens. Spatial Inf. Sci. 42, 339.
Guo, D., Weeks, A., Klee, H., 2004. Segmentations of road area in high resolution images. In: Proceedings of IEEE International Geoscience and Remote Sensing Symposium (IGARSS), vol. 6. IEEE, pp. 3810–3813.
Gupta, S., Girshick, R., Arbeláez, P., Malik, J., 2014. Learning rich features from RGB-D images for object detection and segmentation. In: European Conference on Computer Vision. Springer, pp. 345–360.
Hackel, T., Savinov, N., Ladicky, L., Wegner, J.D., Schindler, K., Pollefeys, M., 2017. Semantic3D.net: A new large-scale point cloud classification benchmark. In: Proceedings of ISPRS Annals of the Photogrammetry, Remote Sensing and Spatial Information Sciences, vol. IV-1-W1, pp. 91–98.
Har-Peled, S., Kumar, N., 2011. Approximate nearest neighbor search for low dimensional queries. In: Proceedings of 22nd Annual ACM-SIAM Symposium on Discrete Algorithms, pp. 854–867.
Hara, K., Le, V., Sun, J., Jacobs, D., Froehlich, J.E., 2013. Exploring early solutions for automatically identifying inaccessible sidewalks in the physical world using google street view. In: Proceedings of Human Computer Interaction Consortium (HCIC).
Hara, K., Sun, J., Moore, R., Jacobs, D., Froehlich, J., 2014. Tohme: Detecting curb ramps in google street view using crowdsourcing, computer vision, and machine learning. In: Proceedings of the 27th Annual ACM Symposium on User Interface Software and Technology (UIST), pp. 189–204.
Hariharan, B., Arbeláez, P., Girshick, R., Malik, J., 2014. Simultaneous detection and segmentation. In: European Conference on Computer Vision. Springer, pp. 297–312.
Hu, H., Munoz, D., Bagnell, J.A., Hebert, M., 2013. Efficient 3-d scene analysis from streaming data. In: 2013 IEEE International Conference on Robotics and Automation. IEEE, pp. 2297–2304.
Illinois Department of Transportation, 2016. Sidewalk network inventory and assessment for the champaign urbana urbanized area. Report no., Illinois Department of Transportation, Champaign-Urbana, Illinois.
Ivan, J.N., Garrick, N.W., Hanson, G., 2009. Designing roads that guides drivers to choose safer speed-final report JHR 09-321. Report No. JHR 09-321, Connecticut Department of Transportation, Rocky Hill, CT.
Jagannathan, A., Miller, E.L., 2007. Three-dimensional surface mesh segmentation using curvedness-based region growing approach. IEEE Trans. Pattern Anal. Mach. Intell. 29 (12), 2195–2204.
Jiang, M., Wu, Y., Zhao, T., Zhao, Z., Lu, C., 2018. Pointsift: A sift-like network module for 3d point cloud semantic segmentation. arXiv preprint arXiv:1807.00652.
Lavoué, G., Dupont, F., Baskurt, A., 2005. A new CAD mesh segmentation method, based on curvature tensor analysis. Comput. Aided Des. 37 (10), 975–987.
Li, H., Cebe, J., Khoeini, S., Xu, Y., Dyess, C., Guensler, R., 2018. A semi-automated method to generate GIS-based sidewalk networks for asset management and pedestrian accessibility assessment. Transp. Res. Rec. 2672 (44), 1–9.
Lin, Y.-J., Benziger, R.R., Habib, A., 2016. Planar-based adaptive down-sampling of point clouds. Photogramm. Eng. Remote Sens. 82 (12), 955–966.
Liu, F., Li, S., Zhang, L., Zhou, C., Ye, R., Wang, Y., Lu, J., 2017. 3dcnn-DQN-RNN: A deep reinforcement learning framework for semantic parsing of large-scale 3D point clouds. In: Proceedings of the IEEE International Conference on Computer Vision. pp. 5678–5687.
Loewenherz, F., 2010. Bellevue's ADA sidewalk and curb ramp compliance program. Washington State LTAP News 1 (103), 6–13.
López Pazos, G., Balado Frías, J., Díaz Vilariño, L., Arias Sánchez, P., Scaioni, M., et al., 2017. Pedestrian pathfinding in urban environments: preliminar results. In: Geospace 2017, Kyiv, Ucrania, 4-6 Diciembre 2017. Enxeñaría dos recursos naturais e medio ambiente.
Lu, X., Yao, J., Tu, J., Li, K., Li, L., Liu, Y., 2016. Pairwise linkage for point cloud segmentation. ISPRS Ann. Photogramm. Remote Sens. Spatial Inf. Sci. 3 (3).
Luo, J., Wu, G., Wei, Z., Boriboonsomsin, K., Barth, M., 2019. Developing an aerial-image-based approach for creating digital sidewalk inventories. Transp. Res. Rec. 0361198119842820.
Ma, L., Li, Y., Li, J., Wang, C., Wang, R., Chapman, M.A., 2018. Mobile laser scanned point-clouds for road object detection and extraction: A review. Remote Sens. 10 (10), 1531.
Maturana, D., Scherer, S., 2015. VoxNet: A 3D convolutional neural network for real-time object recognition. In: Proceedings of IEEE/RSJ International Conference on Intelligent Robots and Systems (IROS), pp. 922–928.
McMahon, P.J., Zegeer, C.V., Duncan, C., Knoblauch, R.L., Stewart, J.R., Khattak, A.J., 2002. An analysis of factors contributing to "walking along roadway" crashes: Research study and guidelines for sidewalks and walkways. Report No. FHWA-RD-01-101, Federal Highway Administration, Washington, D.C..
Meagher, D., 1982. Geometric modeling using octree encoding. Comput. Graph. Image Process. 19 (2), 129–147.
Munoz, D., Bagnell, J.A., Vandapel, N., Hebert, M., 2009. Contextual classification with functional max-margin markov networks. In: 2009 IEEE Conference on Computer Vision and Pattern Recognition. IEEE, pp. 975–982.
New Jersey Department of Transportation, 2007. County road sidewalk inventory, new jersey. https://www.state.nj.us/transportation/refdata/countysidewalks/.
Orhan, M., Dekeyser, G., 2018. Pointnet2 for semantic segmentation of 3d points clouds. GitHub repository.
Qi, C., Hao, S., Mo, K., Guibas, L.J., 2017a. Pointnet: Deep learning on point sets for 3D classification and segmentation. In: Proceedings of IEEE Conference on Computer Vision and Pattern Recognition (CVPR). IEEE, pp. 77–85.
Qi, C.R., Yi, L., Su, H., Guibas, L.J., 2017b. PointNet++: deep hierarchical feature learning on point sets in a metric space. In: Proceedings of Advances in Neural Information Processing Systems, pp. 5099–5108.

Roynard, X., Deschaud, J.-E., Goulette, F., 2018. Paris-Lille-3D: A Large and high-quality ground-truth urban point cloud dataset for automatic segmentation and classification. Int. J. Robot. Res. 37 (6), 545–557.

Sankaranarayanan, J., Samet, H., Varshney, A., 2007. A fast all nearest neighbor algorithm for applications involving large point-clouds. Comput. Graph. 31 (2), 157–174.

Soilán, M., Riveiro, B., Balado, J., Arias, P., 2019. Comparison of heuristic and deep learning-based methods for ground classification from aerial point clouds. Int. J. Digit. Earth 1–20.

Soilan, M., Truong-Hong, L., Riveiro, B., Laefer, D., 2018. Automatic extraction of road features in urban environments using dense ALS data. Int. J. Appl. Earth Obs. Geoinf. 64, 226–236.

Su, H., Jampani, V., Sun, D., Maji, S., Kalogerakis, E., Yang, M.-H., Kautz, J., 2018. Splatnet: Sparse lattice networks for point cloud processing. In: Proceedings of the IEEE Conference on Computer Vision and Pattern Recognition, pp. 2530–2539.

Tan, P., Steinbach, M., Kumar, V., 2005. Introduction To Data Mining. Addison-Wesley.

Tarsha-Kurdi, F., Landes, T., Grussenmeyer, P., 2007. Hough-transform and extended ransac algorithms for automatic detection of 3d building roof planes from lidar data. In: ISPRS Workshop on Laser Scanning 2007 and SilviLaser 2007, vol. 36, pp. 407–412.

Vo, A.-V., Truong-Hong, L., Laefer, D.F., Bertolotto, M., 2015. Octree-based region growing for point cloud segmentation. ISPRS J. Photogramm. Remote Sens. 104, 88–100.

Vosselman, G., Gorte, B.G., Sithole, G., Rabbani, T., 2004. Recognising structure in laser scanner point clouds. Int. Arch. photogramm. Remote Sens. Spatial Inform. Sci. 46 (8), 33–38.

Wu, B., Wan, A., Yue, X., Keutzer, K., 2018. Squeezeseg: Convolutional neural nets with recurrent crf for real-time road-object segmentation from 3d lidar point cloud. In: 2018 IEEE International Conference on Robotics and Automation (ICRA). IEEE, pp. 1887–1893.

Xiao, J., Zhang, J., Adler, B., Zhang, H., Zhang, J., 2013. Three-dimensional point cloud plane segmentation in both structured and unstructured environments. Robot. Auton. Syst. 61 (12), 1641–1652.

Yamauchi, H., Lee, S., Lee, Y., Ohtake, Y., Belyaev, A., Seidel, H.-P., 2005. Feature sensitive mesh segmentation with mean shift. In: International Conference on Shape Modeling and Applications 2005 (SMI'05). IEEE, pp. 236–243.

Ye, X., Li, J., Huang, H., Du, L., Zhang, X., 2018. 3d recurrent neural networks with context fusion for point cloud semantic segmentation. In: Proceedings of the European Conference on Computer Vision (ECCV), pp. 403–417.

Zhang, W., Gupta, S., Lian, X., Liu, J., 2016. Staleness-aware async-SGD for distributed deep learning. In: Proceedings of the Twenty-Fifth International Joint Conference on Artificial Intelligence. In: IJCAI'16, AAAI Press, pp. 2350–2356.

Zhang, X., Li, G., Xiong, Y., He, F., 2008. 3D Mesh segmentation using mean-shifted curvature. In: International Conference on Geometric Modeling and Processing. Springer, pp. 465–474.

Zhou, Q.-Y., Park, J., Koltun, V., 2018. Open3D: A modern library for 3D data processing. arXiv preprint arXiv:1801.09847.

Zhou, B., Zhao, H., Puig, X., Xiao, T., Fidler, S., Barriuso, A., Torralba, A., 2019. Semantic understanding of scenes through the ade20k dataset. Int. J. Comput. Vis. 127 (3), 302–321.